EEG Measurements with Compressed Sensing Utilizing EEG Signals as the Basis Matrix

Daisuke Kanemoto*, and Tetsuya Hirose
Graduate School of Engineering, Osaka University, Suita, Japan
*dkanemoto@eei.eng.osaka-u.ac.jp

***Abstract*—The use of compressed sensing (CS) to achieve low-power consumptions in electroencephalogram (EEG) measurement devices has attracted considerable research interest. However, a signal processing issue in utilizing CS is the trade-off between the compression ratio (CR), reconstruction accuracy, and reconstruction time. In this study, we developed a method that resulted in a shortened reconstruction time and a high reconstruction accuracy with a high CR by utilizing selected EEG signals. When EEG signals were sorted using the mean frequency and only the most frequently occurring EEG signals were used in the basis matrix, a compressed EEG signal with an original time length of 1 s could be recovered in only approximately 26 ms, and an average normalized mean square error of 0.11 was achieved at a CR of 5.**

***Index Terms*—EEG, compressed sensing, BSBL, basis matrix**

I. Introduction

Electroencephalogram (EEG) measurement is a noninvasive technique that has been widely studied owing to its easy acquisition. Therefore, wireless EEG monitoring systems have been increasingly used. Generally, in wireless EEG monitoring systems, the sensors of the sensing unit in a measurement device are placed on the scalp, and the signals are wirelessly transmitted to a data processing unit, such as an edge device or PC, for analysis. It is well-known that for wireless digital data management and exchange, the sensing unit requires a significant amount of power [1]. Therefore, the energy efficiency of the sensing unit is important because its battery life is limited.

The theory of compressed sensing (CS) [2], which is a desirable method for signal acquisition and compression, has attracted significant attention for the realization of a low-power EEG measurement sensing unit [3]–[5]. In general, the compression ratio (CR), reconstruction accuracy, and reconstruction time should be considered when CS is employed. The CR significantly affects power savings in the sensing unit, and the reconstruction accuracy affects the acquired EEG signal quality. In addition, the reconstruction time is a crucial parameter in several practical applications. For example, brain–computer interfaces and brain–machine interfaces require low-power consumption, highly accurate signal acquisition, and a fast response (e.g. [6]). However, a trade-off between the CR, reconstruction accuracy, and reconstruction time hampers the design of measurement systems based on CS [7].

Thus, various studies have been conducted to improve the CS performance. For example, block sparse Bayesian learning (BSBL) [8] is an algorithm that solves the CS problem with high CR and reconstruction accuracy. Thus, it has been employed in several EEG signal acquisition schemes that utilize CS [9]. However, in principle, its computational cost and time consumption are high compared to those of simple algorithms such as orthogonal matching pursuit [10]. Further, in addition to reconstruction algorithms, research on the bases used for sparse representation has also received considerable attention. For example, the K-singular value decomposition (K-SVD) algorithm [11], a basis learning algorithm, has been proposed to generate a basis matrix with sparse representation, and it has subsequently been used in several studies [12]. Moreover, Gabor basis [13] and wavelet basis [14] have been used as basis matrices in the reconstruction of compressed EEG signals. However, such overcomplicated basis matrices tend to increase the reconstruction time because the sizes of the basis matrices increase. In other words, it is desirable to achieve high accuracy with high CR by employing a compact basis matrix such as a discrete cosine transform (DCT) (e.g. [9]). Thus, in this study, we developed a method to realize selected EEG signals as a compact basis matrix appropriate for high-speed reconstruction by relying on the principle of the BSBL algorithm with high CR and reconstruction accuracy.

The remainder of this manuscript is organized as follows. Section Ⅱ briefly describes the CS theory and the study direction. Next, Section Ⅲ explains the proposed method using selected EEG signals as a compact basis matrix. Section Ⅳ presents the effectiveness of the proposed method based on actual EEG signals. Finally, Section Ⅴ presents the conclusions.

II. Background of CS and Directions for This Study

The simple principle underlying CS is explained in the diagram presented in Fig. 1. The CS theory is utilized to obtain a signal vector $\mathbf{x} \in \mathbb{R}^N$, which is k -sparse in a basis matrix $\mathbf{\Psi} \in \mathbb{R}^{N \times P}$. Here, k-sparse implies that only k ($<< P$) elements of the coefficient vector $\mathbf{s} \in \mathbb{R}^P$, which are used to indicate that $\mathbf{x} = \mathbf{\Psi}\ \mathbf{s}$, are nonzero. In this example, $\mathbf{\Psi}$ is represented using a square matrix with $N = P = 10$, and sparsity of $\mathbf{s}$ is

This work was supported by JSPS KAKENHI Grant Number JP21H03410. This paper is based on results obtained from a project, JPNP20004, subsidized by the New Energy and Industrial Technology Development Organization (NEDO).

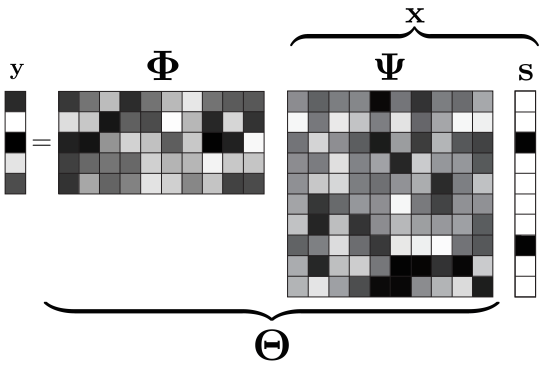

Fig. 1: Compression of the signal $\mathbf{x}$ using the measurement matrix $\mathbf{\Phi}$ to produce a low-dimensional compressed matrix $\mathbf{y}$. The product of $\mathbf{\Phi}$ and $\mathbf{\Psi}$ is termed as the sensing matrix $\mathbf{\Theta}$.

$k = 2$. The color depth indicates the numerical size of each element. The white elements indicate zeros.

We can obtain a compressed signal $\mathbf{y} \in \mathbb{R}^M$ expressed as

$$\mathbf{y} = \mathbf{\Phi x} = \mathbf{\Phi \Psi s} = \mathbf{\Theta s}, \tag{1}$$

where $\mathbf{\Phi}$ is an $M \times N$ measurement matrix. In this study, $\frac{N}{M}$ is defined as the CR; thus, for the $M = 5$ example, the CR = 2. Here, $\mathbf{y}$ is a known vector, and $\mathbf{\Phi}$ and $\mathbf{\Psi}$ are known matrices. Therefore, we can define $\mathbf{\Theta} = \mathbf{\Phi}\ \mathbf{\Psi}$ as a known matrix and label it as the sensing matrix. $\mathbf{\Theta}$ is an important matrix in CS and is the subject of several studies [15]. We can observe that equation (1) is underdetermined because the length of $\mathbf{y}$ is smaller than the length of $\mathbf{s}$. Therefore, several reconstruction algorithms have been applied for solving CS problems by utilizing $\mathbf{\Theta}$ and $\boldsymbol{y}$ to realize a sparse vector $\mathbf{s}$.

In general, $\mathbf{x}$, which is used as a biological signal, has a block/group structure [16]. Subsequently, with an appropriate $\mathbf{\Psi}$, we can assume that $\mathbf{s}$ can be represented by g blocks as

$$\mathbf{s} = [\underbrace{s_1, \cdots, s_{d_1}}_{\mathbf{s}_1^{\mathrm{T}}}, \cdots, \underbrace{s_{d_{g-1}+1}, \cdots, s_{d_g}}_{\mathbf{s}_g^{\mathrm{T}}}]^{\mathrm{T}}. \tag{2}$$

Among the g blocks, only the j ($j \ll g$) blocks are nonzero; however, their locations are unknown. Certain reconstruction algorithms are known to benefit from the structure, as described in [17]. BSBL is a reconstruction algorithm that considers intra-block correlations to further improve the reconstruction accuracy. Thus, numerous studies have been conducted on CS utilizing BSBL. However, its drawback is that the reconstruction is time-consuming compared to that of simple algorithms.

In general, once the $\mathbf{\Phi}$, which depends on the hardware implementation method and the reconstruction algorithm to be used, is determined, the size of $\mathbf{\Psi}$ directly affects the reconstruction time. Therefore, we considered the method of generating the matrix $\mathbf{\Psi}$ with a block structure and the smallest possible size. Furthermore, a complicated method for generating a basis matrix is known to hamper practical applications. Therefore, the proposed method should be simple and easy to use.

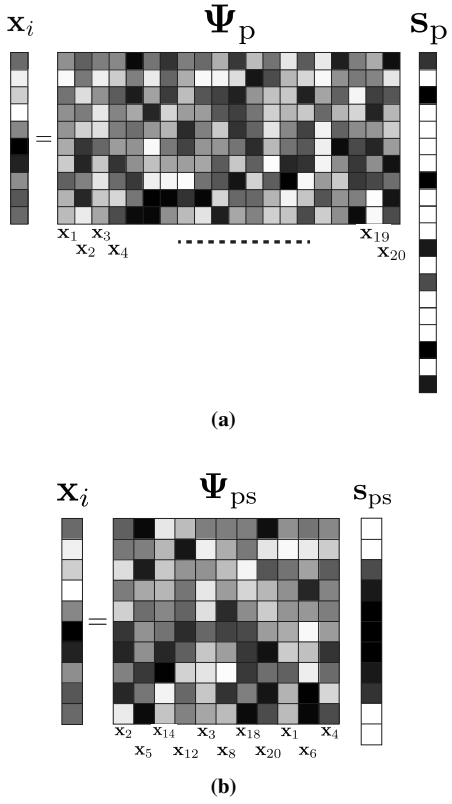

Fig. 2: (a) In several cases, sparsification based on previously acquired biological signals is possible. (b) Compact basis matrix can be realized by selecting highly correlated signals.

III. Proposed Method: Utilizing Selected EEG Signals as a Basis Matrix

Herein, we propose a new basis matrix generation method that is compatible with BSBL and utilizes EEG signals as the basis matrix. A previous study reported that previously obtained EEG signals can be used as the basis matrix [18]. The proposed method also uses EEG signals as the basis matrix; however, reordering and selection are performed to obtain the matrix. The proposed method yields a small-sized basis matrix and efficiently sparsifies the EEG signals for efficient measurements. As an example, details regarding the proposed method are presented in Fig. 2(a) and (b). Figure 2(a) depicts the relationship between an EEG signal $\mathbf{x}_i$ to be measured, the sparse vector $\mathbf{s}_{\mathrm{p}}$, and $\mathbf{\Psi}_{\mathrm{p}}$. For example, the basis matrix created by simply arranging 20 previously obtained EEG signals $\mathbf{x}_1$–$\mathbf{x}_{20}$ is defined as

$$\mathbf{\Psi}_{\mathrm{p}} \stackrel{\mathrm{def}}{=} [\mathbf{x}_1 \mathbf{x}_2 \cdots \mathbf{x}_{20}]. \tag{3}$$

$\mathbf{x}_i$ is not the same signal as the previously obtained signal group. For example, if $\mathbf{x}_i$ is highly correlated with signals $\mathbf{x_1}$ and $\mathbf{x_3}$, the elements corresponding to $\mathbf{x_1}$ and $\mathbf{x_3}$ in $\mathbf{s}_{\mathrm{p}}$ are displayed with large values. The larger the number of EEG signals used, the more likely the presence of highly correlated

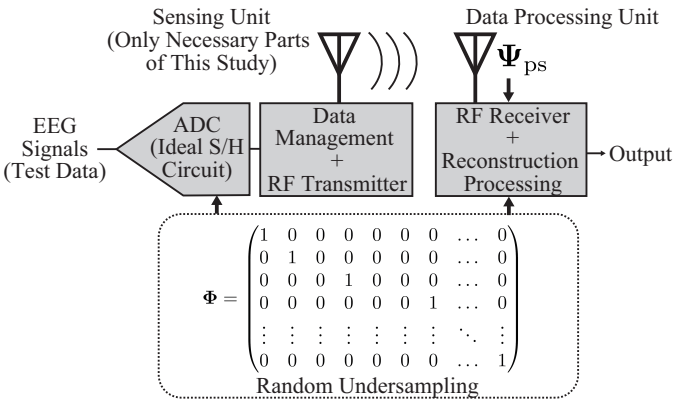

Fig. 3: System used to validate the idea. MATLAB was used for validation, with random undersampling for the ADC and BSBL for reconstruction. An ideal model with no loss of characteristics was assumed for the remainder.

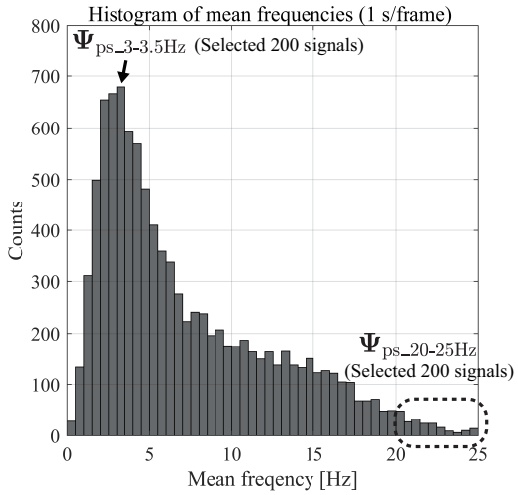

Fig. 4: Histogram of EEG signals with 10,000 frames arranged in terms of their mean frequency and used to generate the basis matrix. Ψ_{all_freq} includes all sorted signals. $\Psi_{ps\_3\text{-}3.5Hz}$ and $\Psi_{ps\_20\text{-}25Hz}$ are the basis matrices comprising the selected top 200 in each mean frequency range.

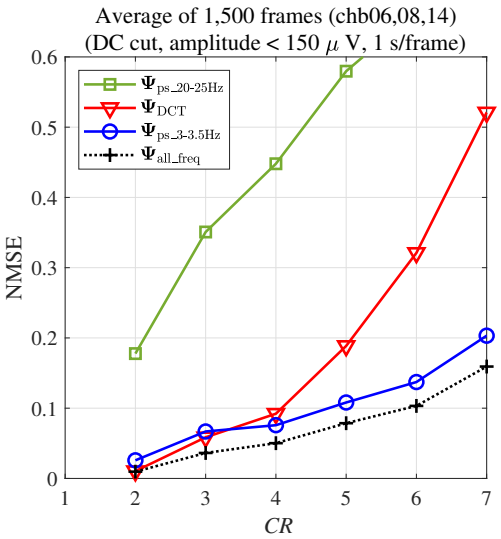

Fig. 5: Relationship between the average NMSE of 1,500 frames and CR when various basis matrices are utilized. The degradations in $\Psi_{ps\_3\text{-}3.5Hz}$ are suppressed at large CRs similar to Ψ_{all_freq}.

elements in the sparse vector. However, the method that uses several EEG signals increases the size of the basis matrix, thus requiring more reconstruction time. Moreover, if $\mathbf{x_1}$–$\mathbf{x_{20}}$ are arranged without regard for each other, the signals highly correlated with $\mathbf{x_i}$ may not be located closely, resulting in the scattering of nonzero element locations in $\mathbf{s_p}$.

Therefore, as illustrated in Fig. 2(b), we develop a method that generates a new basis matrix, Ψ_{ps}. This matrix has a small number of columns and can place the locations of nonzero elements to arbitrary locations in the sparse vector by selecting and rearranging the EEG signals to be used. The $\mathbf{s}_{ps}$ that is achieved using Ψ_{ps} can be suitable for reconstruction using the BSBL algorithm because it can generate blocks of nonzero elements. In this study, the mean frequencies of the $\mathbf{x_1}$–$\mathbf{x_{20}}$ EEG signals were calculated and sorted using the mean frequency values. Note that the number of the basis matrix columns can be reduced by performing selection based on the distribution of the mean frequencies and by focusing on frequencies with a high occurrence rate. For example, in Fig. 2(b), $\mathbf{x_7}$ and $\mathbf{x_9}$ are not included in Ψ_{ps}, indicating that the frequency distribution of the mean frequency was checked, and signals with low occurrence rates were excluded. The proposed method is similar to basis learning algorithms, such as K-SVD, as it uses previously obtained or known signals; however, unlike K-SVD, it does not require complex preprocessing. Thus, it can also reduce the computational load and time required to create the basis matrix.

IV. Evaluation

The effectiveness of the proposed basis matrix used in the EEG measurement was compared with that of the conventional DCT basis matrix. Figure 3 presents a schematic of the simulation system used for this validation, which was built using MATLAB 2022b. Same as in [19], ADC means an ideal sample and hold (S/H) circuit to perform random undersampling in this simulation. Reconstruction processing in the data processing unit was executed using the BSBL algorithm. The other parts were considered as ideal models, because the purpose of this study was to verify the effectiveness of the proposed basis matrix in the reconstruction process.

FP1-F7 channel data, in which seizure symptom periods were avoided, based on the CHB-MIT scalp EEG database were used as test data of EEG signals [20]. The sampling frequency of data was reduced from 256 Hz to 200 Hz, and the time corresponding to one frame was set to 1 s. In this evaluation, a DC component cut was applied to all frames, and frames with an absolute amplitude exceeding 150 μV were simply judged to contain artifacts and excluded. Subsequently, data of the chb06, chb08, and chb14 (each 500 frames) were

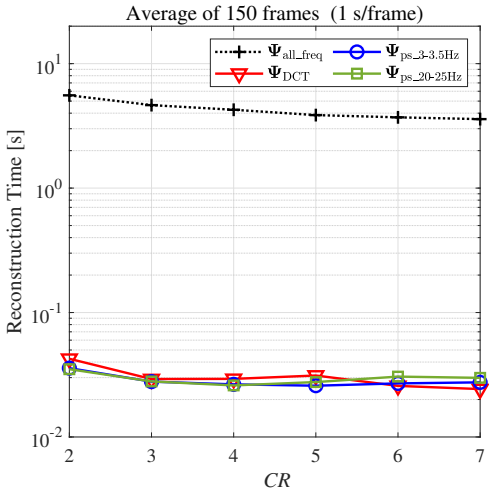

Fig. 6: Relationship between the average reconstruction time and CR when various basis matrices are utilized. $\mathbf{\Psi}_{\text{ps\_3-3.5Hz}}$ has a sufficiently high reconstruction accuracy, which is identical to $\mathbf{\Psi}_{\text{all\_freq}}$; however, the reconstruction time can be significantly reduced, similar to $\mathbf{\Psi_{DCT}}$.

used as test data to perform compression and reconstruction. As shown in Fig. 3, we use a matrix, which consists of only one "1" in each row and zeros in the rest, as the measurement matrix $\mathbf{\Phi} \in \mathbb{R}^{M\times 200}$, to achieve random undersampling [21]. Effectiveness of random undersampling for implementation has been discussed as low power consumption [22]. The validity of the reconstruction accuracy was confirmed for 1,500 frame averages of EEG signals, and a fair and statistical check could be performed.

The previously obtained EEG signals for generating $\mathbf{\Psi}$ were chb01, 02, 03, 04, and 05 (each 2,000 frames), which were different from the subject of the test signal and were prepared by the same process as the test data. The mean frequency distribution of the previously obtained signal (10,000 frames) is shown in Fig. 4. There was a bias specific to EEG signals. In this evaluation, the basis matrix taking advantage of this characteristic was used. The following basis matrices were considered in this verification: DCT (200 columns) as $\mathbf{\Psi}_{\text{DCT}} \in \mathbb{R}^{200\times 200}$, a matrix generated by sorting all signals in ascending order based on their mean frequency as $\mathbf{\Psi}_{\text{all\_freq}} \in \mathbb{R}^{200\times 10{,}000}$, and a matrix $\mathbf{\Psi}_{\text{ps\_3-3.5Hz}} \in \mathbb{R}^{200\times 200}$ created by retrieving the signals with mean frequencies between 3 Hz and 3.5 Hz from $\mathbf{\Psi}_{\text{all\_freq}}$ and extracting the top 200 signals. To confirm the accuracy of this reconstruction when the basis matrix was created using signals with low histogram counts, a matrix $\mathbf{\Psi}_{\text{ps\_20-25Hz}} \in \mathbb{R}^{200\times 200}$ was also constructed using the signals with the top 200 mean frequencies from 20 Hz to 25 Hz as the basis matrix.

In this study, the index of the normalized mean square error (NMSE) was used as follows:

$$\text{NMSE} = \frac{\|\mathbf{x} - \hat{\mathbf{x}}\|_2^2}{\|\mathbf{x}\|_2^2}, \tag{4}$$

where $\mathbf{x}$ is the original EEG signal and $\hat{\mathbf{x}}$ is the reconstructed EEG signal. The DC component of $\hat{\mathbf{x}}$ was also removed before calculating the NMSE. The smaller the value of the NMSE, the higher the accuracy of the reconstruction. In this evaluation, BSBL was used as the reconstruction algorithm, and g was set to 30. The value of g was the same for all basis cases because it is known to affect both the reconstruction accuracy and time, and 30 was the value with the highest reconstruction accuracy when the DCT basis was used.

Figure 5 presents the relationship between the average NMSE of 1,500 frames and CR when $\mathbf{\Psi}_{\text{DCT}}$, $\mathbf{\Psi}_{\text{ps\_3-3.5Hz}}$, $\mathbf{\Psi}_{\text{ps\_20-25Hz}}$, and $\mathbf{\Psi}_{\text{all\_freq}}$ are utilized. The results reveal that the reconstruction resulting from $\mathbf{\Psi}_{\text{ps\_20-25Hz}}$ was poor compared to that resulting from the other bases. Therefore, it is not suitable to use a signal with a low occurrence count as a basis. It was also discovered that no significant difference exists between $\mathbf{\Psi}_{\text{DCT}}$, $\mathbf{\Psi}_{\text{ps\_3-3.5Hz}}$, and $\mathbf{\Psi}_{\text{all\_freq}}$ when the CR is low. However, as the CR increases, $\mathbf{\Psi}_{\text{DCT}}$ presents the highest NMSE. $\mathbf{\Psi}_{\text{all\_freq}}$ and $\mathbf{\Psi}_{\text{ps\_3-3.5Hz}}$ yielded approximately the same results. In other words, even when using $\mathbf{\Psi}_{\text{ps\_3-3.5Hz}}$, which is a compact matrix compared to $\mathbf{\Psi}_{\text{all\_freq}}$, the performance approaches to that of $\mathbf{\Psi}_{\text{all\_freq}}$. Specifically, an NMSE value of 0.11 can be achieved at CR = 5 with $\mathbf{\Psi}_{\text{ps\_3-3.5Hz}}$, although an NMSE of 0.19 is obtained with conventional basis $\mathbf{\Psi_{DCT}}$.

A computer with an Intel Core i7 CPU and 16 GB RAM was employed to record the average time required to perform the reconstruction. Figure 6 presents the results of selecting 150 frames from chb06, chb08, and chb14 when $\mathbf{\Psi}_{\text{DCT}}$, $\mathbf{\Psi}_{\text{ps\_3-3.5Hz}}$, $\mathbf{\Psi}_{\text{ps\_20-25Hz}}$, and $\mathbf{\Psi}_{\text{all\_freq}}$ are used. The reconstruction time is almost identical when using $\mathbf{\Psi}_{\text{DCT}}$, $\mathbf{\Psi}_{\text{ps\_3-3.5Hz}}$, and $\mathbf{\Psi}_{\text{ps\_20-25Hz}}$, which have the same number of columns; however, $\mathbf{\Psi}_{\text{all\_freq}}$, which has a larger number of columns, takes longer to process. The results indicate that the reconstruction time is not significantly affected by the CR; however, it varies considerably depending on the number of columns. The reconstruction time $\mathbf{\Psi}_{\text{ps\_3-3.5Hz}}$ can be significantly reduced to 26 ms owing to the small number of columns, although $\mathbf{\Psi}_{\text{ps\_3-3.5Hz}}$ is approximately the same as $\mathbf{\Psi}_{\text{all\_freq}}$ considering the reconstruction accuracy.

V. Conclusions

Herein, we developed a new compact basis matrix generation method that utilized previously obtained EEG signals and evaluated its effectiveness based on MATLAB calculations. By analyzing the trend followed by the mean frequency of the previously acquired EEG signals and using the most frequently occurring EEG signals in the basis matrix, we achieved a reconstruction time of only 26 ms for an EEG signal with a time of 1 s at CR = 5 while maintaining the average NMSE at approximately 0.11. Our results are expected to further expand the application scope of CS for EEG signals because the results of this study can be used to resolve the conventional trade-offs in EEG measurements by applying CS.

REFERENCES

[1] J. V. Assche and G. Gielen, "Power efficiency comparison of event-driven and fixed-rate signal conversion and compression for biomedical applications," *IEEE Trans. Biomed. Circuits Syst.*, vol. 14, no. 4, pp. 746–756, Jul. 2020.

[2] D. L. Donoho, "Compressed sensing," *IEEE Trans. Inf. Theory,* vol. 52, no. 4, pp. 1289–1306, Apr. 2006.

[3] A. M. Abdulghani, A. J. Casson, and E. Rodriguez-Villegas, "Compressive sensing scalp EEG signals: implementations and practical performance," *Med. Biol. Eng. Comput.*, vol. 50, pp. 1137–1145, Sep. 2011.

[4] M. Khosravy, N. Dey, and C. A. Duque, *Compressive Sensing in Healthcare.* Academic Press, 2020.

[5] S. Katsumata, D. Kanemoto, and M. Ohki, "Applying outlier detection and independent component analysis for compressed sensing EEG measurement framework," in *Proc. IEEE Biomed. Circuits Syst. Conf. (BioCAS)*, Oct. 2019, pp. 1–4.

[6] T.-H. Nguyen, D.-L. Yang, and W.-Y. Chung, "A high-rate BCI speller based on eye-closed EEG signal," *IEEE Access,* vol. 6, pp. 33995-34003, Jun. 2018.

[7] D. Gurve, D. Delisle-Rodriguez, T. Bastos-Filho, and S. Krishnan, "Trends in compressive sensing for EEG signal processing applications," *Sensors,* vol. 20, no. 13, pp. 3703–3723, Jul. 2020.

[8] Z. Zhang, and B. D. Rao, "Extension of SBL algorithms for the recovery of block sparse signals with intra-block correlation," *IEEE Trans. Signal Process.,* vol. 61, no. 8, pp. 2009–2015, Apr. 2013.

[9] Z. Zhang, T.-P. Jung, S. Makeig, and B. D. Rao, "Compressed sensing of EEG for wireless telemonitoring with low energy consumption and inexpensive hardware," *IEEE Trans. Biomed. Eng.,* vol. 60, no. 1, pp. 221–224, Jan. 2013.

[10] T. T. Cai and L. Wang, "Orthogonal matching pursuit for sparse signal recovery with noise," *IEEE Trans. Inf. Theory,* vol. 57, no. 7, pp. 4680–4688, Jul. 2011.

[11] M. Aharon, M. Elad, and A. Bruckstein, "K-SVD: An algorithm for designing overcomplete dictionaries for sparse representation," *IEEE Trans. Signal Process.,* vol. 54, no. 11, pp. 4311–4322, Nov. 2006.

[12] K. Nagai, D. Kanemoto, and M. Ohki, "Applying K-SVD dictionary learning for EEG compressed sensing framework with outlier detection and independent component analysis," *IEICE Trans. Fundamentals*, vol. E104-A, no. 9, pp. 1375–1378, Sep. 2021.

[13] M. Mohsina and A. Majumdar, "Gabor based analysis prior formulation for EEG signal reconstruction," *Biomed. Signal Process. Control*, vol. 8, no. 6, pp. 951–955, Nov. 2013.

[14] L. Lin, Y. Meng, J. P. Chen, and Z. B. Li, "Multichannel EEG compression based on ICA and SPIHT," *Biomed. Signal Process. Control*, vol. 20, pp. 45–51, Jul. 2015.

[15] M. Mangia, F. Pareschi, V. Cambareri, R. Rovatti, and G. Setti, *Adapted Compressed Sensing for Effective Hardware Implementations*. Springer, 2018.

[16] Y. C. Eldar, P. Kuppinger, and H. Bölcskei, "Block-sparse signals : uncertainty relations and efficient recovery," *IEEE Trans. Signal Process,* vol. 58, no. 6, pp. 3042–3054, Jun. 2010.

[17] R. G. Baraniuk, V. Cevher, M. F. Duarte, and C. Hegde, "Model-based compressive sensing," *IEEE Trans. Inf. Theory,* vol. 56, no. 4, pp. 1982–2001, Apr. 2010.

[18] M. Fira, and L. Goras, "Comparison of inter-and intra-subject variability of P300 spelling dictionary in EEG compressed sensing," *Int. J. Adv. Comput. Sci. Appl.,* vol. 7, no. 10, pp. 366–371, 2016.

[19] D. Kanemoto, S. Katsumata, M. Aihara, and M. Ohki, "Framework of applying independent component analysis after compressed sensing for electroencephalogram signals," in *Proc. IEEE Biomed. Circuits Syst. Conf. (BioCAS)*, Oct. 2018, pp. 145–148.

[20] A. Shoeb, Application of Machine Learning to Epileptic Seizure Onset Detection and Treatment. *PhD Thesis, Massachusetts Institute of Technology*, Sep. 2009.

[21] M. Trakimas, R. D'Angelo, S. Aeron, T. Hancock, and S. Sonkusale, "A compressed sensing analog-to-information converter with edge triggered SAR ADC core," *IEEE Trans. Circuits Syst. I, Reg. Papers,* vol. 60, no. 5, pp. 1135–1148, Apr. 2013.

[22] Y. Okabe, D. Kanemoto, O. Maida, and T. Hirose, "Compressed Sensing EEG Measurement Technique with Normally Distributed Sampling Series," *IEICE Trans. Fundamentals,* vol. E105-A, no.10, pp. 1429-1433, Oct. 2022.